Composites Science and Technology 153 (2017) 232–240

Contents lists available at ScienceDirect

Composites Science and Technology

journal homepage: http://www.elsevier.com/locate/compscitech

Orientation-dispersed pseudo-ductile hybrid composite laminates – A new lay-up concept to avoid free-edge delamination

Meisam Jalalvand [a, b, *], Mohamad Fotouhi [b, c], Michael R. Wisnom [b]

[a] Department of Mechanical and Aerospace Engineering, University of Strathclyde, 75 Montrose Street, Glasgow, G1 1XJ, UK
[b] Bristol Composites Institute (ACCIS), University of Bristol, Queen's Building, University Walk, Bristol, BS8 1TR, UK
[c] Department of Design and Mathematics, The University of the West of England, Bristol, BS16 1QY, UK

ARTICLE INFO

Article history:
Received 21 April 2017
Received in revised form
10 October 2017
Accepted 14 October 2017
Available online 17 October 2017

Keywords:
Hybrid composites
Fragmentation
Non-linear behaviour
Stress/strain curves
Finite Element Analysis (FEA)

ABSTRACT

Multi-Directional hybrid composites can suffer from free-edge delamination, a damage mode that doesn't exist in Uni-Directional hybrid composites and can hinder the pseudo-ductility that can be achieved with thin-ply hybrids. This paper presents a new lay-up concept called '*orientation-dispersed*' laminates to avoid this mode of damage in quasi-isotropic hybrids. It is shown that the energy release rates at the free-edges of orientation-dispersed layups are significantly lower than those in '*orientation-blocked*' laminates. Finally, the experimental results from two quasi-isotropic layups with $\pi/3$ and $\pi/4$ intervals are presented showing a good pseudo-ductility with no free-edge delamination.

1. Introduction

Conventional composites usually exhibit a catastrophic failure with no prior warning. This has led to conservative design and large reserve factors in the design of composite structures and also frequent expensive health-monitoring checks during operation. Pseudo-ductility is a relatively new concept proposed to address such difficulties. In this approach, the possible failure processes are divided into two categories of favourable gradual and unfavourable catastrophic damage modes. By designing a composite to exhibit the desirable failure modes and avoiding the fatal ones, it is possible to achieve gradual deterioration and stiffness reduction while keeping the integrity and load carrying capacity of the laminate.

Hybridisation with thin plies is one of the successful methods to achieve gradual failure or pseudo-ductility [1,2]. In this method, two types of plies with different fibres and failure strains are co-cured to achieve fragmentation of the lower strain material and a gradual stiffness reduction during this process. Early work on hybrid composites dates back to the 1970s when hybridisation was reported to be a good way to enhance the failure strain of carbon fibres in glass/carbon hybrids [3–8] and also to achieve a more cost-effective material [9,10]. Showing a gradual failure, a higher toughness and pseudo-ductility are other potential advantages of hybrids compared to brittle non-hybrid composites if they are well designed [4,7,11–15]. Mixing the fibres can be done in different levels such as intermingled continuous fibres [16], intermingled aligned short fibres [17], interlayer or sandwiched layers [18] and intralayer [19]. Glass/carbon [4,13,18],carbon/carbon [20–22] and polymer fibre/carbon [19,23] are some of the common material combinations used in hybrid composites.

Four different types of failure processes have been recognised for Uni-Directional (UD) hybrid composites [24,25]: 1) premature high strain material failure after the first crack in the low strain material, 2) catastrophic delamination of the low strain material from the high strain material after the first crack in the low strain material, 3) fragmentation of the low strain material and 4) fragmentation of the low strain material followed by limited dispersed delamination. The first two failure modes are unfavourable and should be avoided because they result in catastrophic failure of the composite and lead to mechanical properties lower than the constituents. Damage Mode Maps were found to be a useful way to achieve optimum UD hybrids with the favourable failure process of

* Corresponding author. Department of Mechanical and Aerospace Engineering, University of Strathclyde, 75 Montrose Street, Glasgow, G1 1XJ, UK.
E-mail addresses: m.jalalvand@strat.ac.uk, jalalvand.meisam@gmail.com (M. Jalalvand).

https://doi.org/10.1016/j.compscitech.2017.10.011
0266-3538/

fragmentation in the low strain material [26].

Most of the work done to-date on hybrid composites has concerned UD hybrids and only a limited number of papers have studied multi-directional hybrids [22,27]. But UD composites are not widely applied in real-life applications because of their poor transverse properties, so multi-directional laminates such as Quasi-Isotropic (QI) ones are normally used. To achieve a successful pseudo-ductile multi-directional laminate, it is important to distinguish the differences between the failure processes of uni- and multi-directional laminates.

While the favourable and unfavourable failure modes for multi-directional and quasi-isotropic hybrid composites are similar to those in UD hybrids, multi-directional and QI ones have one important extra failure mode which does not take place in UD ones: free-edge delamination.

Free-edge delamination is an unfavourable mode of failure in QI hybrids that may occur even before fibre fragmentation in the low strain material and hinder achieving pseudo-ductility. It also causes loss of laminate integrity and can lead to premature catastrophic failure or significant load drops [28] if it occurs after fragmentation initiation. Elastic modulus, toughness and thickness of the plies plus the layup and stacking sequence of the laminate all greatly contribute to the occurrence of this mode of failure [29]. For hybrid laminates, the complexity of the problem is even greater as dispersion of the low and high strain layers through the thickness can also influence the delamination load.

In this paper, the concept of 'orientation-dispersed' stacking sequence to avoid free-edge delamination is proposed and compared with 'orientation-blocked' published earlier [27]. It will be shown that the energy release rates are significantly lower in the orientation-dispersed laminates and therefore, the possibility of such failure is greatly reduced. The proposed concept is finally proved by experimental results on QI glass/carbon hybrids with $\pi/3$ and $\pi/4$ layer orientation intervals.

2. Concept

The orientation-blocked stacking sequence pseudo-ductility concept, previously published in Ref. [27], is based on using UD hybrid sub-laminates with the low strain material layer embedded in between two high strain material layers with similar fibre orientation. UD hybrid configurations were optimised using the Damage Mode Map analytical design tool [26], and then used as the building block for the QI hybrids with different fibre orientations i.e. 0, ±45 and 90. Fig. 1 (a) shows a schematic example of an orientation-blocked quasi-isotropic glass/carbon hybrid with stacking sequence $[45_H/90_H/\text{-}45_H/0_H]_S$. H stands for Hybrid and means that each layer is a sandwich of two high and one low strain material layers. The layup is colour-coded based on the fibre type in each layer in Fig. 1 (a): yellow for the high strain material e.g. glass/epoxy and grey for the low strain material e.g. carbon/epoxy.

If we change the way this layup is coloured and use fibre angle as the parameter to separate different layers, the stacking sequence would look like Fig. 1 (b) with four different colours for the different angles of 45, 90, −45, 0. While Fig. 1 (a) shows that the high and low strain materials are well dispersed through the thickness, Fig. 1 (b) indicates rather thick blocks with the same fibre orientation through the thickness. This is the reason, we used the term 'orientation-blocked' for this layup.

The main concept in the 'orientation-dispersed' layup is that the layers with similar fibre angle are evenly distributed through the thickness. In other words, the emphasis in dispersion is put on fibre orientation rather than on material type. Fig. 2 indicates an orientation-dispersed hybrid laminate, equivalent to that shown in Fig. 1. The laminate is coloured based on fibre type in Fig. 2 (a), the low strain and high strain materials are segregated and there are rather thick blocks of each. However, colour separation based on fibre angle as shown in Fig. 2 (b), indicates that the fibre orientation is well dispersed through the thickness. The lower thickness of the blocks with similar fibre orientation in this laminate compared against those in Fig. 1 (b) suggests a lower risk of free-edge delamination. This is quite similar to previous studies with non-hybrid materials where layups with similar stacking sequences but with thinner plies have showed a significantly higher strain to delamination initiation [30]. In addition to free-edge delamination, the transverse-cracking initiation strain also depends on the thickness of each sub-laminate, so orientation-dispersed layups can postpone transverse cracking initiation as well.

It is worth mentioning that orientation-dispersed laminates can be optimised at the QI level, assuming homogenised properties for each QI material. For instance, the QI high and low strain materials in the orientation-dispersed laminate shown in Fig. 2 (a) can be assumed to be homogeneous and as a result, the damage mode map technique can be directly applied to find the optimum configurations of each QI layer. More details on this can be found in Ref. [31].

3. Finite Element Analysis

Free edge delamination is dependent on the interlaminar energy release rate (G) at the free-edges. To calculate these values, a Finite Element (FE) model along with the Virtual Crack Closure Technique (VCCT) is used. Individual layers are separately modelled using 3D 8-noded brick elements (C3D8I) to find the full stress state including all interlaminar stresses causing delamination in the Abaqus V6.14. Far away from the end tabs, the stress state does not vary along the length of the specimen, so a generalised plane strain solution can be applied to avoid modelling the full length of a specimen. For this purpose, the 'slice-modelling' method discussed in Ref. [32] is used.

Fig. 3 indicates a slice of an orientation-blocked hybrid laminate with a 2 mm initial crack between the 90 and -45 high strain material layers. To achieve the uniform deformation far away from the end-tabs, each node on the back surface is constrained to have displacements in the transverse and thickness directions exactly equal to those of the counterpart node on the front surface. To assure constant strain in the loading direction along the x axis, the difference of the movement of the corresponding nodes should be equal to the extension of the slice (x-direction strain, ε, multiplied by the slice's x-direction dimension L). For instance, point A is on the front surface and A' is marked on the back surface in Fig. 3. To achieve the correct 3D stress and strains far away from the end-tabs, the constraints in Equation (1) were applied using the *Equation multi-point constraints in Abaqus for pairs of nodes with the same y and z coordinates on the back and front surface e.g. A and A'.

$$\begin{aligned} u_A - u_{A'} &= \varepsilon L \\ v_A - v_{A'} &= 0 \\ w_A - w_{A'} &= 0 \end{aligned} \tag{1}$$

In the slice modelling technique, only one row of element along the x direction is usually required for stress and strain analysis. But in this study, the energy release rate (G) values are calculated using the VCCT, which relies on the nodal forces and displacements. Since application of the constraints in Equation (1) will result in extra nodal forces either on the back or front surface nodes, a minimum of two element rows are required along the x-direction to have nodes which are not directly constrained through Equation (1). Therefore, the nodal forces and displacements at the tip of the crack are captured from the node(s) not on the constrained front and

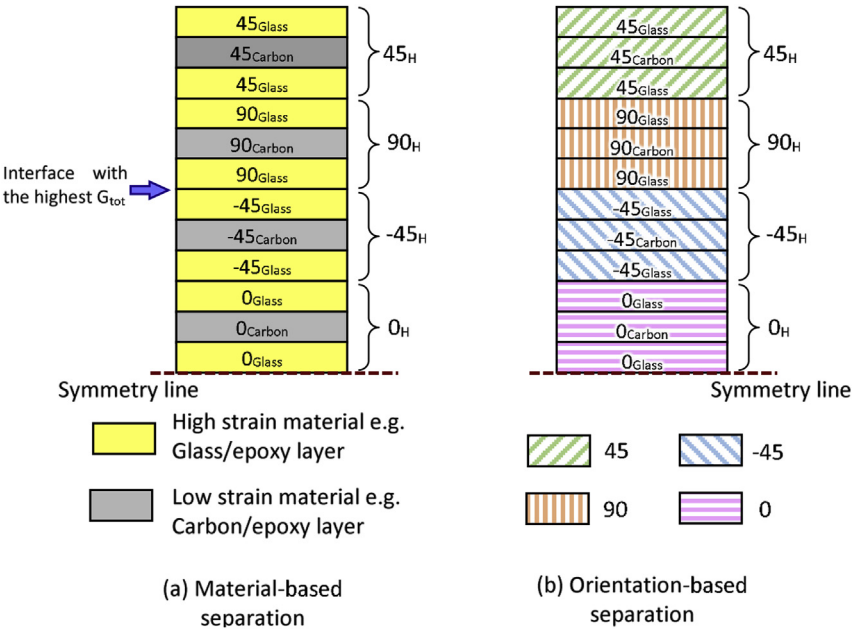

Fig. 1. Orientation-blocked stacking sequence with (a) material-based and (b) orientation-based colour separation. (For interpretation of the references to colour in this figure legend, the reader is referred to the web version of this article.)

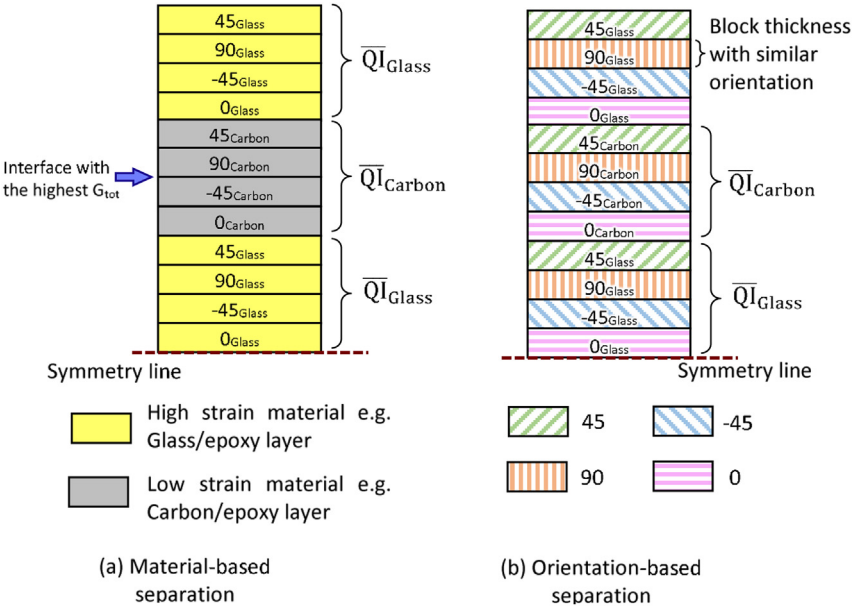

Fig. 2. Orientation-dispersed stacking sequence with (a) material-based and (b) orientation-based colour separation. (For interpretation of the references to colour in this figure legend, the reader is referred to the web version of this article.)

back surfaces, but from the nodes inside the slice.

The Abaqus built-in VCCT subroutine was used to calculate the energy release rates. To validate the implementation of this subroutine, a new in-house Python function for calculating the energy release rates using the VCCT was also developed and the obtained results found to be very similar to those from the Abaqus subroutine.

As both orientation-blocked and orientation-dispersed layups are quasi-isotropic with similar ratios of glass to carbon, they have similar moduli and thermal expansion coefficients. Therefore, the effect of thermal residual stresses is assumed not to be very different and they were not taken into account.

3.1. Energy release rate (G) values

Two separate FE models of orientation-blocked and orientation-dispersed hybrid laminates with similar hybrid material combinations are studied in this part to show the importance of stacking sequence. Previously, UD T1000/XN80 hybrid composites had been tested [21] and showed a good pseudo-ductile response. The same UD hybrid sub-laminate was later used as the building block of a QI orientation-blocked laminate [27] with the stacking sequence shown in Fig. 1. The failure process in this multi-directional laminate started with fragmentation of the low strain material (XN80 carbon epoxy layer) in the 0 layer at a strain of about 0.4% and then

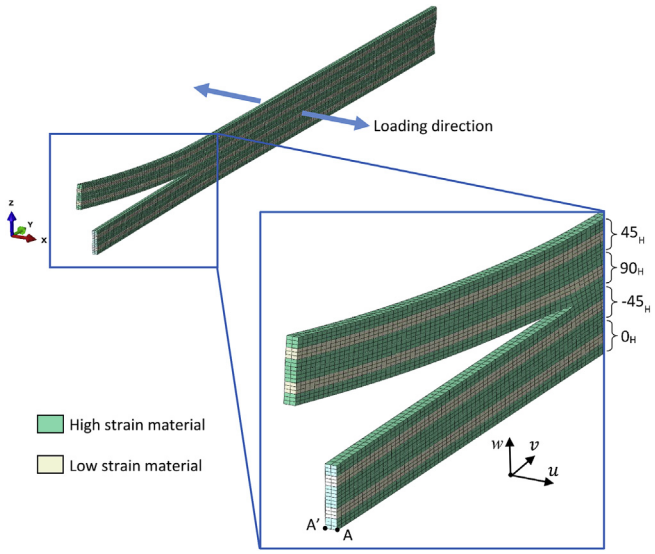

Fig. 3. 3D slice of a blocked orientation hybrid laminate with an initial crack between the 90_H/-45_H interface -displayed deformation is 10 times the original one.

turned into free-edge delamination at 0.8% strain, well before the final failure strain.

The FE slice modelling method was used to calculate the energy release rates for this orientation-blocked laminate (Fig. 1) as well as for the new orientation-dispersed stacking sequence concept shown schematically in Fig. 2. The energy release rates depend on which interface is considered as the delaminating one during the VCCT analysis and also on the delamination length. Therefore, the total energy release rates, equal to the sums of all G components ($G_{tot} = G_I + G_{II} + G_{III}$) have been calculated for different crack lengths at all 11 interfaces of both orientation-blocked and orientation-dispersed laminates. The FE results showed that for both laminates, the G_{tot} values depend on the length of delamination only at crack lengths lower than 2 mm and at longer cracks, G_{tot} approaches a constant value. Fig. 4 indicates this variation of G_{tot} for different delamination lengths at the 6th interface (tagged as the 'interface with the highest G_{tot}' in Figs. 1 and 2).

To find the interfaces at which delamination would potentially propagate, the steady values of G_{tot} for delamination lengths of 5 mm at all interfaces are shown in Fig. 5 (a) for both orientation-blocked and orientation-dispersed laminates. The mixed-mode ratios, shown in Fig. 5 (b), defined as the ratio of shear to total energy release rates $(G_{II} + G_{III})/G_{tot}$ are quite similar at all interfaces and in both layups and vary between 79% and 100% showing that delamination is shear dominated and the total energy release rate is a plausible way to make an initial comparison of all different cases.

Clearly, the G_{tot} values are significantly larger in the orientation-blocked laminate at interfaces number 2–7, and also the mode I components are larger (the mixed-mode ratio is lower). The maximum G_{tot} for both laminate occurs at the interface number 6 where the G_{tot} = 0.19 N/mm for the orientation-dispersed and G_{tot} = 0.59 N/mm for the orientation-blocked one. This means that the energy release rate for the orientation-dispersed layup is less than a third of that for the orientation-blocked one. Such a significant 68% reduction in energy release rate of the orientation-dispersed laminates means that the strains at which free-edge delamination initiate are significantly higher and therefore, the possibility of getting free-edge delamination is significantly reduced.

4. Experiments

4.1. Materials

XN80 Pitch-based carbon fibres used in the previous study [21] suffer from a low compressive failure strain of about 0.14% so it was decided to change to a fibre which has a good failure strain in both tension and compression. The materials considered in the experimental part of this study are SkyFlex USN020A thin carbon prepreg from SK Chemicals and standard thickness S-glass/913 epoxy prepreg supplied by Hexcel. The characteristics of the prepregs are listed in Table 1. The carbon fibres in the USN020A were T300 from Toray and the corresponding matrix was SK Chemical's type K50 epoxy. The resin systems in the hybrid laminates were 120 °C cure epoxies, which were found to be compatible with each other in previous experiments [33]. Table 1 shows the elastic modulus of the layers. The mechanical properties of the USN020A prepreg layers were previously measured on the same product with a similar fibre type [34] and for the S-glass/913 epoxy, the transverse properties were assumed to be equal to E-glass/913 prepreg as the fibre volume fracttion in both prepregs are similar and no data was available for the S-glass/epoxy prepreg.

4.2. Layup selection

In the previous comprehensive experimental study on UD hybrid composites [18], it was shown that for the $[0_G/0_{C2}/0_G]$ layup, a sandwich of one Hexcel S-Glass on either side and 2 embedded

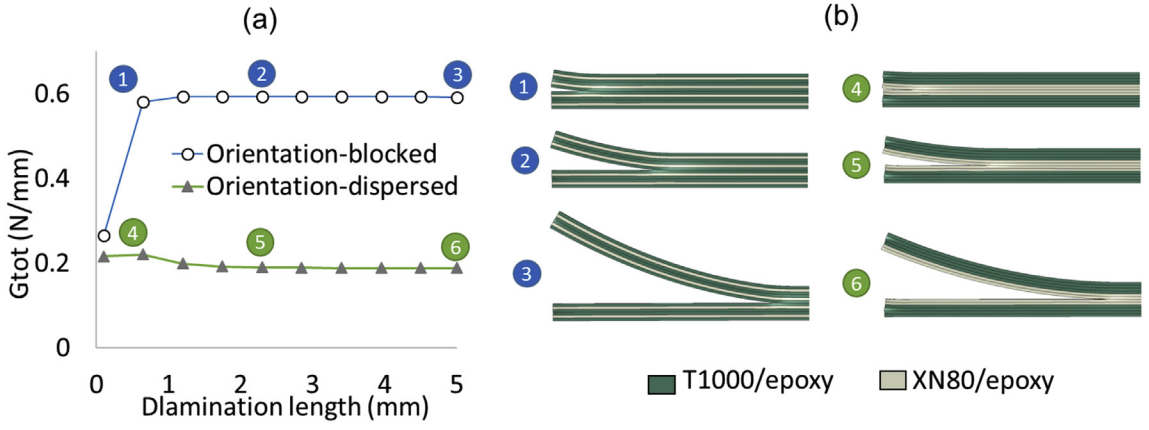

Fig. 4. (a) Total energy release rate (G_{tot}) of the orientation-blocked and orientation-dispersed laminates with different delamination lengths at the most susceptible interface.

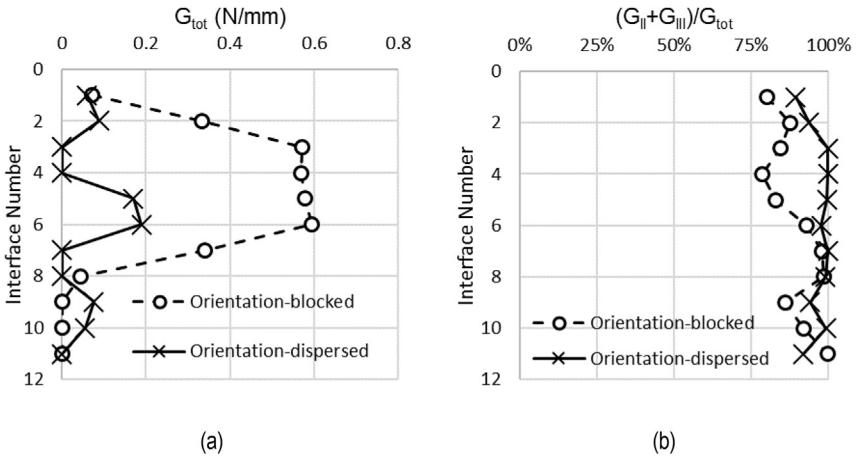

Fig. 5. (a) Total energy release rate (G_{tot}) and (b) mix-mode ratio, ($G_{II} + G_{III}$)/Gtot, for crack length of 5 mm at a far-field strain of 1% for both orientation-blocked and orientation-dispersed layups with T1000/XN80 hybrid combination.

Table 1
Characteristics of the prepregs and fibres used.

Prepreg type	Fibre type	Fibre modulus (GPa)	Fibre failure strain (%)	Cured nominal thickness (mm)	Fiber mass per unit area (g/m2)	Fibre volume fraction (%)	E1 (GPa)	E2 (GPa)	G12 (GPa)	υ12
Hexcel S-glass/913 [18]	S2 glass	88	5.5	0.155	190	51	45.6	15.4[a]	4.34[a]	0.3[a]
SK Chemicals USN020A [18]	T300 – Toray[b]	230	1.5[b]	0.029	21	41	101.7	6.0	2.4	0.3

[a] Assumed to be equal to E-glass properties used in Ref. [24].
[b] This value is based on [36] as the fibre in the applied USN020A prepreg was different from that in Ref. [18].

USN020A thin Carbon layers in the middle, was the most promising configuration. Fig. 6 indicates the stress-strain response of 4 different layups of [$0_G/0_{Cm}/0_G$], (m = 1–3) and [$0_{G2}/0_{C4}/0_{G2}$] where SG and TR30 stands for 0_G and 0_C respectively. Obviously, those layups with 3 and 4 carbon plies suffer from a sharp load drop at the first carbon layer fracture due to catastrophic delamination propagation. The [$0_G/0_{C2}/0_G$], layup shows a better stiffness and broader plateau compared to [$0_G/0_{C1}/0_G$], as well. Therefore, this carbon/glass ratio is used in this study.

The selected base stacking sequence for the quasi-isotropic laminate is [45/90/-45/0]s, which is a common layup and similar to the previous work [27] with the 90 layers away from the mid-plane, avoiding a thick ply block susceptible to transverse cracking. For this material combination, the orientation-blocked concept to achieve a quasi-isotropic pseudo-ductile composite laminate would be [$45_G/45_{C2}/45_G/90_G/90_{C2}/90_G/-45_G/-45_{C2}/-45_G/0_G/0_{C2}/0_G/]_S$, similar to Fig. 1. But based on the new concept of orientation-dispersed lay-up presented in this paper, free-edge delamination could be suppressed using this layup: [$45_G/90_G/-45_G/0_G/45_{C2}/90_{C2}/-45_{C2}/0_{C2}/45_G/90_G/-45_G/0_G]_S$. The comparison of total energy release rates, G_{tot}, for these orientation-blocked and -dispersed laminates for a 5 mm crack at different interfaces and with a remote strain of 1% is shown in Fig. 7 (a). The highest G_{tot} value in the orientation-blocked laminate is 0.16 N/mm whereas it is only 0.035 N/mm in the orientation-dispersed version. To take the effect of the mixed-mode ratio into account, the failure index, defined as $G_I/G_{Ic} + (G_{II} + G_{IIIc})/G_{IIc}$ is shown in Fig. 7 (b). Typical values of 0.2 and 1.0 N/mm were used for GIc and GIIc respectively. For the orientation-blocked laminate, the maximum failure index at this particular strain is 0.29 at the 5th interface whereas it is only 0.06 at the second interface in the orientation dispersed laminate. This clearly shows that the expected initiation strain for free-edge delamination is more than double in the orientation-dispersed laminate compared to the latter one.

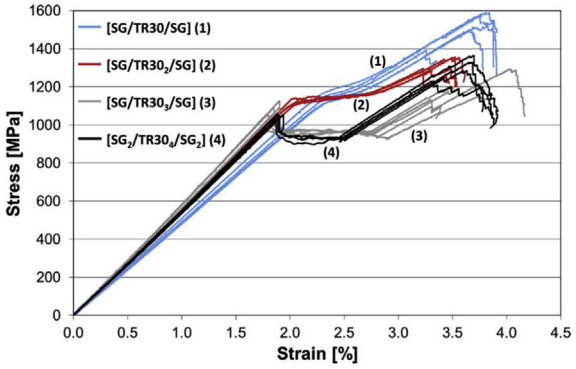

Fig. 6. Tensile stress–strain graphs of S-glass/USN020A carbon configurations [18].

Another interesting aspect of using orientation-dispersed laminates is that they offer more flexibility in-terms of achieving symmetric laminates with lower total laminate thickness. For example, if the initially suggested orientation-dispersed laminate is split at the mid-plane, it is not possible to achieve a symmetric laminate even after shuffling different hybrid sub-laminates. However, in the orientation-dispersed laminate, it is possible to achieve symmetry with half the total number of layers after some subtle layer rearrangements. So the initial orientation-dispersed laminate in Fig. 2 can be easily modified to [$45_G/90_G/-45_G/0_G/(45_C/90_C/-45_C/0_C)_S/0_G/-45_G/-90_G/45_G]_S$ only by shuffling the carbon and glass layers. Since half of this layup is still symmetric, we can reduce the number of layers and only manufacture [$45_G/90_G/-45_G/0_G/45_C/90_C/-45_C/0_C]_S$ and still obtain a similar failure process. Using such a layup with half the thickness halves the consumed material

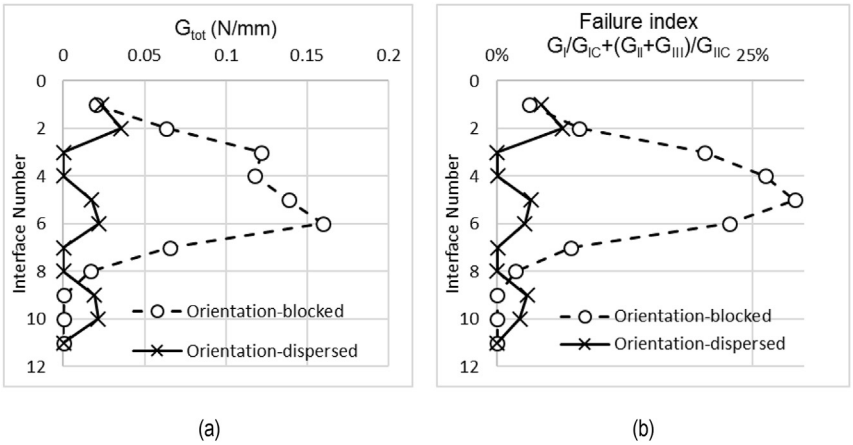

Fig. 7. (a) Total energy release rate (G_{tot}) and (b) Failure index for mixed-mode ratio, $G_I/G_{Ic} + (G_{II} + G_{III})/G_{IIc}$, for crack length of 5 mm at a far-field strain of 1% for both orientation-blocked and orientation-dispersed layups with S-glass/USN020A carbon hybrid combination.

and reduces the time for manufacturing test specimens. Such a thickness reduction was not possible to achieve with orientation-blocked laminates due to symmetry constraints. More importantly, the minimum thickness of the orientation-dispersed layups is half that of orientation-blocked ones. So in real applications, the final selected layup can be more optimal and closer to the required design thickness with orientation-dispersed layups.

Our final choice of layup was slightly different: $[45_G/90_G/-45_G/0_G/0_C/45_C/90_C/-45_C]_S$ to separate the two 0 carbon layers and put them away from the mid-plane. The main idea for such a layup was to avoid fragmentation in the double 0_C layers followed by breaking the off-axis carbon layers which potentially might lead to catastrophic delamination. With the two 0_C layers separated, the finally tested layup, $[45_G/90_G/-45_G/0_G/0_C/45_C/90_C/-45_C]_S$, is more likely to achieve pseudo-ductility and gradual failure than the standard orientation-dispersed layup $[45_G/90_G/-45_G/0_G/45_C/90_C/-45_C/0_C]_S$. FE results approved that the energy release rates for this layup at fibre failure strain will be still low so the risk of free edge delamination stays negligible.

A 300 mm × 300 mm plate with the selected layup, $[45_G/90_G/-45_G/0_G/0_C/45_C/90_C/-45_C]_S$, was manufactured using Hexcel S-glass and SkyFlex USN020A carbon prepregs. After trimming 10 mm off the edges, 50 mm end-tabbing strips made out of cross-ply glass/epoxy laminates were bonded to either side of the ends. The plate with bonded end-tabs were then cut into 20 mm wide specimens with about 200 mm free length. The overall extension was measured using an Imetrum videogauge over a 160 mm gauge length.

4.3. Tensile test results – QI laminates with 45° intervals

The obtained tensile response of the 6 different specimens with orientation-dispersed quasi-isotropic hybrid laminate $[45_G/90_G/-45_G/0_G/0_C/45_C/90_C/-45_C]_S$ is shown in Fig. 8. The stress-strain curves can be divided into four zones: 1) linear elastic with minor damage such as matrix cracking in the off-axis layers, 2) fragmentation of the 0 carbon layers, 3) dispersed delamination at the 0 carbon layer interfaces plus extra damage in the off-axis layers and 4) 0 glass-layer failure. The important achievement is that the stress-strain curves show a good pseudo-ductile response without any load drop before the final failure, whereas typical non-hybrid ones show little nonlinearity before the first significant load drop [28].

Fig. 9 shows a photograph of a loaded specimen just before its final failure point. The lines along the 45° angle indicate transverse

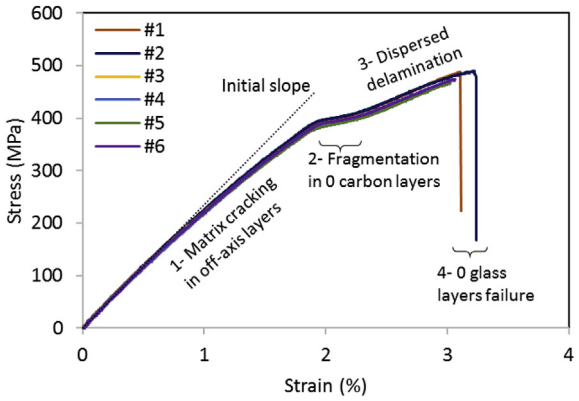

Fig. 8. Tensile stress-strain curves of the orientation-dispersed hybrid quasi-isotropic laminate $[45_G/90_G/-45_G/0_G/0_C/45_C/90_C/-45_C]_S$.

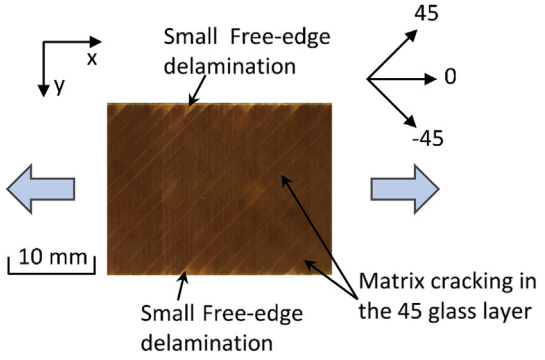

Fig. 9. Photograph from the top of the $[45_G/90_G/-45_G/0_G/0_C/45_C/90_C/-45_C]_S$ orientation-dispersed quasi-isotropic hybrid laminate just before final failure showing almost no free-edge delamination.

cracking in the surface layer. The small bright triangles at the edge of the specimen shown with small arrows indicate that the edge delamination is very small and is bounded by matrix cracks in the surface 45 layer at the edge. Free-edge delamination has been well suppressed and has not led to any interim load-drop. This highlights the advantage of the orientation-dispersed concept over the orientation-blocked layups presented in Ref. [27], where free-edge delamination was fully developed well before the final failure of the

high strain material and led to an undulating stress-strain curve with considerable load drops.

The initial slope line is also drawn with a dashed line. The deviation from this line before the carbon fibre failure strain is due to transverse cracks in the off-axis layers, 90, 45 and −45. This is because the failure strain of the carbon fibres is 1.6% and only transverse cracks could occur before fragmentation in the 0 carbon layer.

Fig. 10 (a) indicates specimen #1 after it has been removed from the grips of the testing machine. The failure has occurred in the gauge section far away from the tabs. This is typically the case in hybrid composites due to suppression of the stress-concentration at the end-tabs and can be generally difficult to achieve in non-hybrids where failure usually initiates close to the end tab [35]. To observe the damage mode in the 0 carbon layer, a part of the broken top glass layer was carefully lifted and removed from the specimen as shown in Fig. 10 (b). The oblique hatch-like pattern in the black carbon layer in this figure is the fragmentation pattern in the 0 carbon ply. The transverse cracks in the 45, 90 and −45 glass layers are also highlighted. Please note that the 0 glass layer was cut with scissors to access the 0 carbon layer and the clear cut in the 0 glass layer was not due to the applied testing load. A more magnified image of the fragmentation in the 0 carbon layer is shown in Fig. 11, using optical microscopy.

4.4. QI laminates with 60° intervals

The same concept can be applied to achieve quasi-isotropic hybrid laminates with 60° fibre orientation intervals. The layup based on the orientation-dispersed concept shown in Fig. 2 is $[60_G/\text{-}60_G/0_G/60_C/\text{-}60_C/0_C]_S$. However, similarly to the previous layup, it was decided to avoid double 0 carbon layers in the mid-plane so the final selected layup was $[60_G/\text{-}60_G/0_G/0_C/60_C/\text{-}60_C]_S$. Fig. 12 indicates the obtained stress-strain responses of 5 tested specimens with this layup. The obtained curves are very similar to those with 45° intervals discussed in section 4.3. Similarly to before, four regions with different damage modes are labelled in this figure: 1) elastic region with minor matrix cracking in the ±60 layers, 2) fragmentation of the 0 carbon layers, 3) dispersed delamination between 0 carbon fragments and surrounding layers and 4) finally 0 glass layer fibre failure.

The FE slice model of this layup was also built and the maximum

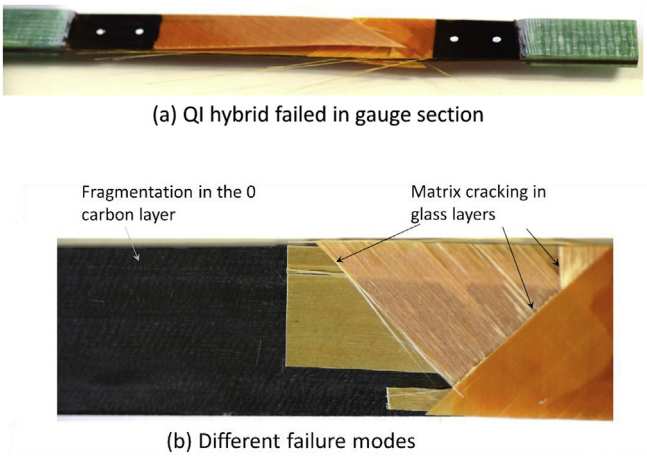

Fig. 10. (a) Specimen #1 failed in the gauge section, (b) Transverse matrix cracking in the glass layers and fragmentation in the 0 carbon layer after removing some parts of the surface glass– Note that the 0 glass layer was cut with scissors to show the fragmented carbon layer underneath.

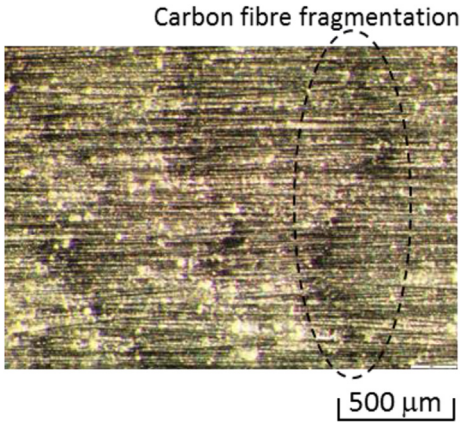

Fig. 11. Optical microscopy image from the top view of the 0 carbon layer showing the fragments.

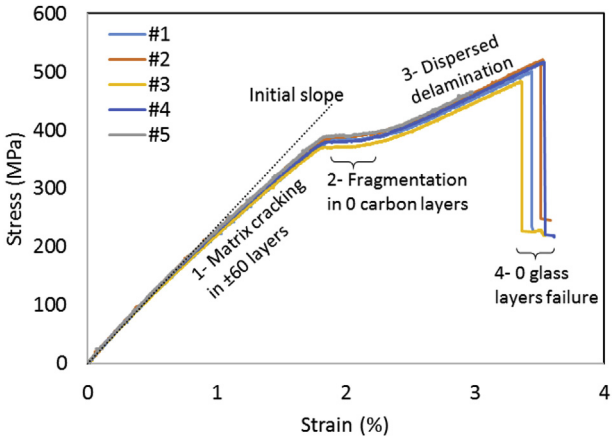

Fig. 12. Stress-strain curves of $[60_G/\text{-}60_G/0_G/0_C/60_C/\text{-}60_C]_S$ specimens.

energy release rate at 1% tensile strain was found to be only 0.00087 N/mm, which is only 2% of the Gtot = 0.04 N/mm for the orientation-dispersed quasi-isotropic laminate with 45° fibre orientation intervals. Therefore, no free-edge delamination was expected for this laminate at all. The obtained experimental results fully confirmed this prediction.

5. Comparison and discussion

The obtained stress-strain curves are very different from typical non-hybrid standard quasi-isotropic materials such as those reported in Ref. [28]. Normally, non-hybrid composites have a linear-elastic stress-strain curve up until a significant sudden load drop or their final failure. But both quasi-isotropic laminates presented in this paper showed a good nonlinear metal-like stress-strain curve with about 1% pseudo-ductile strain before their final failure. This is because a gradual and evenly distributed fibre failure was achieved over the whole specimen and free-edge delamination as a fatal damage mode was avoided.

The response of two typical Quasi-Isotropic (QI) specimens with 45° and 60° ply fibre orientation intervals, $[45_G/90_G/\text{-}45_G/0_G/0_C/45_C/90_C/\text{-}45_C]_S$ and $[60_G/\text{-}60_G/0_G/0_C/60_C/\text{-}60_C]_S$, are compared in Fig. 13. The initial part of the curve associated with elastic response of the layers with minor matrix cracking is identical and the curves overlay. However, the knee points and the average plateau stresses are slightly different. The average knee point strain for the QI

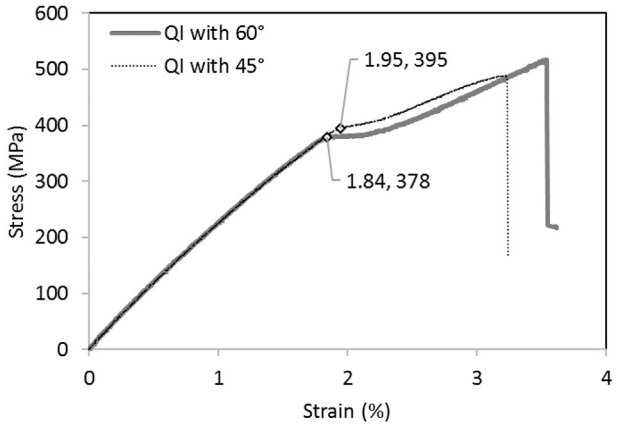

Fig. 13. Comparison of the stress-strain response of the orientation-dispersed quasi-isotropic laminates with layers of 45° and 60° angle intervals.

laminate with 60° interval layers is 1.84% whereas for the other one, it is 1.95%. These two values are significantly higher than the manufacturer's quoted 1.5% failure strain for T300 fibres [36] and 1.6% knee point fragmentation strain in another pseudo-ductile configuration with angle-ply blocks around the 0 plies [37]. This enhancement in the failure strain of the 0 carbon layer is due to the 'hybrid effect', which has recently been studied in UD thin-ply specimens [38] and a 20% increase was reported for a single thin 30 g/m^2 SkyFlex TR30 layer embedded between two standard thickness UD Hexcel S-glass layers, [$0_G/0_C/0_G$]. The knee point strain in the quasi-isotropic laminate with 45° intervals, 1.95%, is 22% higher than the fibre fragmentation strain, 1.6% [37]. This suggests that the hybrid effect in [$45_G/90_G/-45_G/0_G/0_C/45_C/90_C/-45_C]_S$ may be similar to that in the [$0_G/0_C/0_G$] UD hybrid laminate reported in Ref. [38]. It was previously shown that the strain enhancement is strongly dependent on the ply thickness in UD hybrids. The thickness of single 0 carbon plies in both these quasi-isotropic laminates is the same, however they are separated by different carbon/epoxy sub-laminates. The two 0 carbon layers in the quasi-isotropic layup with 45° intervals are separated with a 6-layer sub-laminate, [$45_C/90_C/-45_C/-45_C/90_C/45_C$]. However, for the other quasi-isotropic laminate with 60° intervals, the two 0 carbon layers are separated with only a 4-layer sub-laminate of [$60_C/-60_C/-60_C/60_C$] which is thinner, less strong and less stiff compared to [$45_C/90_C/-45_C/-45_C/90_C/45_C$]. The difference between the separating layers is believed to influence the extent of the hybrid effect. The separated 0 carbon layers can have more interaction in the QI with 60 intervals. This is because the stress concentration due to fragmentation in one 0 carbon layer can more easily lead to failure in the other layer in this QI laminate with a thinner and lower stiffness separating sub-laminate compared to the other QI with 45° intervals.

Assuming the mechanical properties for the USN020 thin carbon layer given in Ref. [24], $E_1 = 101.7$ GPa, E2 = 6 GPa, and G12 = 2.4 GPa, we can compare the stiffness of the two laminates separating the two 0 carbon layers. The modulus of the [$60_C/-60_C/-60_C/60_C$] sub-laminate along the 0 direction is 5880 MPa so the stiffness of this sub-laminate is 682 N/mm (E_x multiplied by the thickness). For [$45_C/90_C/-45_C/-45_C/90_C/45_C$], the modulus is 16449 MPa and the stiffness is 2862 N/mm, which is 4.2 times the stiffness of the previous sub-laminate. Therefore, the [$45_C/90_C/-45_C/-45_C/90_C/45_C$] layup is a much stiffer barrier between the two 0 carbon layers, taking much more load compared to the [$60_C/-60_C/-60_C/60_C$] sub-laminate. As a result, although the 0 carbon layers are physically separated from each other in this quasi-isotropic laminate, their fragmentation process may not be fully independent and there may be some interaction between the two 0 carbon layers.

Fig. 14 shows the fragmentation pattern of the 0 carbon layers in both quasi-isotropic laminates over the whole width of the samples. Clearly, the crack density in the QI laminate with 45° intervals is higher than that in the laminates with 60° intervals. The average fragmentation spacing in the QI laminate with 60° intervals is approximately 1.1 mm but in the other laminate, it is 0.7 mm. This is consistent with the argument on the effect of the stiffness and strength of the sub-laminate separating the two 0 carbon layers. The thinner sub-laminate in the 60° interval case leads to more interaction between the layers, and hence greater fragmentation spacing and lower hybrid effect.

The fragmentation lines are not normal to the loading direction and have an oblique pattern with a slight tendency towards the adjacent layer fibre orientation. The reason for this is not yet fully understood and further analysis is planned to study this effect.

The final failure strain of these two laminates have a meaningful difference. The quasi-isotropic laminate with 45° intervals has an average failure strain of 3.1% and the other one fails at 3.5% in average. Final failure takes place when the 0 glass layers are broken. So this difference can be related to the ratio of the 0 glass layer to the overall thickness. In the quasi-isotropic laminate with 45° intervals, the thickness of 0 glass layers is 21% of the total thickness whereas in the one with 60° intervals, 0 glass layers comprise 28% of the total thickness. So it is reasonable to expect that the quasi-isotropic laminates with 60° intervals should be stronger than those with 45° intervals.

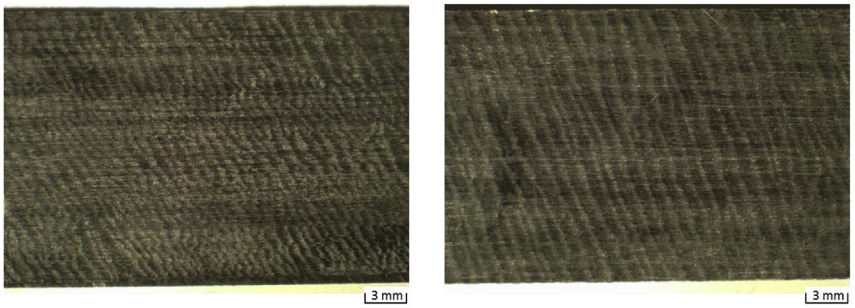

Fig. 14. Fragmentation pattern in the 0 carbon layer of the orientation-dispersed quasi-isotropic layers [$45_G/90_G/-45_G/0_G/0_C/45_C/90_C/-45_C]_S$ and [$60_G/-60_G/0_G/0_C/60_C/-60_C]_S$ after removing the surface glass layers.

6. Conclusions

The new concept of orientation-dispersed stacking sequences was proposed to avoid free-edge delamination in achieving multi-directional/quasi-isotropic pseudo-ductile hybrid laminates. This concept was applied to two different quasi-isotropic layups with 45° and 60° fibre angle intervals. The energy release rates for free-edge delamination found through using a FE slice model were almost a quarter of those for orientation-blocked laminates. No significant free-edge delamination was observed in the experiments, proving that the lay-up concept is successful in suppressing free-edge delamination.

The obtained pseudo-ductile stress-strain curves are completely different from those achieved from conventional non-hybrid composites which suffer from a brittle failure. The laminates showed a high plateau stress without any load drop before the final failure.

The stress-strain response of both quasi-isotropic laminates with 45° and 60° fibre angle intervals were quite similar, with high pseudo-yield stresses and strains and also final strength. The small difference in the knee points in these two laminates is related to the difference in the hybrid effect. In the laminate with 45° fibre angle intervals, the 0 carbon layers are separated with a thicker, stronger and stiffer sub-laminate compared to the other one. Therefore, the 0 carbon layers fragment similarly to individual carbon layers embedded in a high strain material. But in the other laminate, the $[\pm 60]_S$ plies in between the 0 carbon layers are not strong and stiff enough, so the fragmentation in the 0 carbon layers may interact. This is supported by the longer fragmentation spacing in this laminate compared to the quasi-isotropic with 45° fibre angle intervals.

Acknowledgment

This work was funded under the UK Engineering and Physical Sciences Research Council Programme Grant EP/I02946X/1 on High Performance Ductile Composite Technology in collaboration with Imperial College, London. The authors acknowledge Hexcel Corporation for supplying materials for this research. The data necessary to support the conclusions is included in the paper.

References

[1] Y. Swolfs, L. Gorbatikh, I. Verpoest, Fibre hybridisation in polymer composites: a review, Compos Part A Appl. Sci. Manuf. 67 (2014) 181–200.
[2] G. Czél, M.R. Wisnom, Demonstration of pseudo-ductility in high performance glass-epoxy composites by hybridisation with thin-ply carbon prepreg, Compos Part A Appl. Sci. Manuf. 52 (2013) 23–30.
[3] T. Hayashi, K. Koyama, A. Yamazaki, M. Kihira, Development of new material properties by hybrid composition, Fukugo Zair, Compos. Mater 1 (1972) 18–20.
[4] A.R. Bunsell, B. Harris, Hybrid carbon and glass fibre composites, Composites 5 (1974) 157–164.
[5] J. Aveston, J.M. Sillwood, Synergistic fibre strengthening in hybrid composites, J. Mater Sci. 11 (1976) 1877–1883.
[6] C. Zweben, Tensile strength of hybrid composites, J. Mater Sci. 12 (1977) 1335–1337.
[7] P.W. Manders, M.G. Bader, The strength of hybrid glass/carbon fibre composites, J. Mater Sci. 16 (1981) 2233–2245.
[8] C.C. Chamis, R.F. Lark, J.H. Sinclair, Mechanical property characterization of interply hybrid composites, in: Am. Soc. Test. Mater. Symp, 1979. Dearborn, Michigan.
[9] D. Short, J. Summerscales, Hybrids-a review: Part 1, Tech. Des. Constr. Compos. (1979) 215–222.
[10] P.T. Curtis, M. Browne, Cost-effective high performance composites, Composites 25 (1994) 273–280.
[11] J. Aveston, A. Kelly, Theory of multiple fracture of fibrous composites, J. Mater Sci. 8 (1973) 352–362.
[12] H.G. Harris, W. Somboonsong, F.K. Ko, New ductile hybrid FRP reinforcing bar for concrete structures, J. Compos Constr. 2 (1998) 28–37.
[13] D. Short, J.S. Es, Hybrids, A review - Part 2. Physical properties, Composites (1980) 33–38.
[14] R. Alessi, F. Freddi, Phase-field modelling of failure in hybrid laminates, Compos Struct. 181 (2017) 9–25.
[15] R. Alessi, J. Ciambella, A. Paolone, Damage evolution and debonding in hybrid laminates with a cohesive interfacial law, Meccanica 52 (2017) 1079–1091.
[16] H. Diao, A. Bismarck, P. Robinson, M.R. Wisnom, Production of continuous intermingled CF/GF hybrid composite via fibre tow spreading technology, in: Eccm16-16Th Eur Conf Compos Mater, 8, 2014.
[17] H. Yu, M.L. Longana, M. Jalalvand, M.R. Wisnom, K.D. Potter, Pseudo-ductility in intermingled carbon/glass hybrid composites with highly aligned discontinuous fibres, Compos Part A Appl. Sci. Manuf. 73 (2015) 35–44.
[18] G. Czél, M. Jalalvand, M.R. Wisnom, Design and characterisation of advanced pseudo-ductile unidirectional thin-ply carbon/epoxy–glass/epoxy hybrid composites, Compos Struct. 143 (2016) 362–370.
[19] Y. Swolfs, L. Crauwels, Breda E. Van, L. Gorbatikh, P. Hine, I. Ward, et al., Tensile behaviour of intralayer hybrid composites of carbon fibre and self-reinforced polypropylene, Compos Part A Appl. Sci. Manuf. 59 (2014) 78–84.
[20] K. Naito, Tensile properties of polyacrylonitrile- and pitch-based hybrid carbon fiber/polyimide composites with some nanoparticles in the matrix, J. Mater Sci. 48 (2013) 4163–4176.
[21] Czél G, Jalalvand M, Wisnom MR, Czigány T. Design and characterisation of high performance, pseudo-ductile all-carbon/epoxy unidirectional hybrid composites. Compos Part B Eng n.d.
[22] R. Amacher, J. Cugnoni, J. Brunner, E. Kramer, C. Dransfeld, W. Smith, et al., Toward aerospace grade thin-ply composites, in: Proc ECCM-17, 17th Eur Conf Compos Mater, 2016.
[23] A. Pegoretti, E. Fabbri, C. Migliaresi, F. Pilati, Intraply and interply hybrid composites based on E-glass and poly(vinyl alcohol) woven fabrics: tensile and impact properties, Polym. Int. 53 (2004) 1290–1297.
[24] M. Jalalvand, G. Czél, M.R. Wisnom, Numerical modelling of the damage modes in UD thin carbon/glass hybrid laminates, Compos Sci. Technol. 94 (2014) 39–47.
[25] M. Jalalvand, G. Czél, M.R. Wisnom, Damage analysis of pseudo-ductile thin-ply UD hybrid composites - a new analytical method, Compos Part A Appl. Sci. Manuf. 69 (2015) 83–93.
[26] M. Jalalvand, G. Czél, M.R. Wisnom, Parametric study of failure mechanisms and optimal configurations of pseudo-ductile thin-ply UD hybrid composites, Compos Part A Appl. Sci. Manuf. 74 (2015) 123–131.
[27] G. Czél, T. Rév, M. Jalalvand, M. Fotouhi, M.L. Longana, O.J. Nixon-Pearson, M.R. Wisnom, Pseudo-ductility and reduced notch sensitivity in multi-directional all-carbon/epoxy thin-ply hybrid composites. Composites PartA (Accepted).
[28] M.R. Wisnom, B. Khan, S.R. Hallett, Size effects in unnotched tensile strength of unidirectional and quasi-isotropic carbon/epoxy composites, Compos Struct. 84 (2008) 21–28.
[29] T.K. O'brien, Characterization of delamination onset and growth in a composite laminate, Damage Compos Mater ASTM STP (1982) 140–167.
[30] S. Sihn, R.Y. Kim, K. Kawabe, S.W. Tsai, Experimental studies of thin-ply laminated composites, Compos Sci. Technol. 67 (2007) 996–1008.
[31] M. Fotouhi, M. Jalalvand, M.R. Wisnom, High performance quasi-isotropic thin-ply carbon/glass hybrid composites with pseudo-ductile behaviour in all fibre orientations, Compos Sci. Technol. 152 (2017) 101–110.
[32] W. Jiang, J.L. Henshall, Analysis of composite laminate beams using coupling cross-section finite element method, Appl. Math. Mech. 27 (2006) 1709–1718.
[33] M. Jalalvand, G. Czél, J.D. Fuller, M.R. Wisnom, L.P. Canal, C.D. González, et al., Energy dissipation during delamination in composite materials - an experimental assessment of the cohesive law and the stress-strain field ahead of a crack tip, Compos Sci. Technol. 134 (2016) 115–124.
[34] J. Fuller, M.R. Wisnom, Damage suppression in thin ply angle-ply carbon/epoxy laminates, in: 19th Int. Conf. Compos. Mater, 2013. Montreal.
[35] G. Czél, M. Jalalvand, M.R. Wisnom, Hybrid specimens eliminating stress concentrations in tensile and compressive testing of unidirectional composites, Compos Part A Appl. Sci. Manuf. 91 (2016) 436–447.
[36] T300 Data Sheet - No. CFA-001. n.d.
[37] X. Wu, J.D. Fuller, M.R. Wisnom, Open-hole response of pseudo-ductile thin-ply angle-ply laminate, in: 17th Eur. Conf. Compos. Mater, 2016. Munich.
[38] M.R. Wisnom, G. Czél, Y. Swolfs, M. Jalalvand, L. Gorbatikh, I. Verpoest, Hybrid effects in thin ply carbon/glass unidirectional laminates: accurate experimental determination and prediction, Compos Part A Appl. Sci. Manuf. 88 (2016) 131–139.